HAL
open science

Width dependent collisionless electron dynamics in the static fields of the shock ramp, 1, Single particle behavior and implications for downstream distribution

M. Gedalin, M. A. Balikhin

▶ To cite this version:

M. Gedalin, M. A. Balikhin. Width dependent collisionless electron dynamics in the static fields of the shock ramp, 1, Single particle behavior and implications for downstream distribution. Nonlinear Processes in Geophysics, 1997, 4 (3), pp.167-172. hal-00301856

HAL Id: hal-00301856
https://hal.science/hal-00301856

Submitted on 18 Jun 2008

HAL is a multi-disciplinary open access archive for the deposit and dissemination of scientific research documents, whether they are published or not. The documents may come from teaching and research institutions in France or abroad, or from public or private research centers.

L'archive ouverte pluridisciplinaire **HAL**, est destinée au dépôt et à la diffusion de documents scientifiques de niveau recherche, publiés ou non, émanant des établissements d'enseignement et de recherche français ou étrangers, des laboratoires publics ou privés.

Nonlinear Processes in Geophysics (1997) 4: 167–172

Nonlinear Processes in Geophysics
© European Geophysical Society 1997

Width dependent collisionless electron dynamics in the static fields of the shock ramp, 1, Single particle behavior and implications for downstream distribution

M. Gedalin[1] **and M.A. Balikhin**[2]

[1]Ben-Gurion University, Beer-Sheva, Israel
[2]Sheffield University, Sheffield, England

Received: 26 August 1997 – Accepted: 26 February 1998

Abstract. We study the collisionless dynamics of electrons in the shock ramp using the numerical trajectory analysis in the model electric and magnetic fields of the shock. Even with very modest assumptions about the cross-shock potential the electron trajectories are very sensitive to the width of the ramp. The character of electron motion changes from the fully adiabatic (with conservation of $v_\perp^2/B$) when the ramp is wide, to the nonadiabatic one, when the ramp becomes sufficiently narrow. The downstream electron distribution also changes drastically, although this change depends on the initial electron temperature.

1 Introduction

Electron dynamics in the shock front (at least within the ramp) is usually thought to be collisionless (see for the review Scudder, 1995, and references therein). Knowledge of the details of this dynamics and of the downstream electron distribution, which is produced collisionlessly in the ramp, is essential for any model of electron heating in the shock front. The most popular model proposed for explanation of electron heating in shocks (see Feldman, 1985, and references therein) suggests that electrons are accelerated along the magnetic field lines by the cross-shock electric field adiabatically, that is, $v_\perp^2/B = \text{const}$. The de Hoffman-Teller potential is then responsible for the increase of the parallel energy, which dominates. The collisionless part of the downstream distribution function can be written immediately using the magnetic moment and energy conservation:

$$v_\perp^2 = v_{\perp 0}^2(B/B_0), \qquad v^2 = v_0^2 + 2e\phi^{(HT)}/m_e, \qquad (1)$$

Correspondence to: Department of Physics, Ben-Gurion University, P.O. Box 653, Beer-Sheva, 84105, Israel

which gives

$$f(v_\parallel, v_\perp) = f_0((v_{\parallel 0}, v_{\perp 0})\theta(\epsilon_\parallel), \qquad (2)$$

$$v_\perp = v_\perp\sqrt{B/B_0}, \qquad (3)$$

$$v_\parallel = \sqrt{\epsilon_\parallel}\,\mathrm{sign}(v_{\parallel 0}), \qquad (4)$$

$$\epsilon_\parallel = v_{\parallel 0}^2 + 2e\phi^{(HT)}/m_e + v_{\perp 0}^2(1 - B/B_0), \qquad (5)$$

$$\theta(x) = (1 + \mathrm{sign}(x))/2. \qquad (6)$$

This collisionless acceleration produces a large gap in the distribution function. For example, for $v_{\perp 0} = 0$ one finds $v_{\parallel,\min} = \sqrt{2e\phi^{(HT)}/m_e}$. This gap should be filled due to some processes other than the described adiabatic acceleration. In the original version of the mechanism the gap filling and isotropization of the downstream electron distribution is assumed to be due to some pre-existing electron population (Feldman, 1985). Later approaches bring into focus instabilities (Veltri et al., 1990; Veltri and Zimbardo, 1993a,b; Scudder, 1995) or simply assume that the nature is wise enough to find the right way to do that. It is worth mentioning that the above collisionless mapping for $v_\perp = 0$ was used to estimate the de Hoffman-Teller cross-shock potential (Schwartz et al., 1988).

Another scenario was proposed for electron heating in thin shocks (Balikhin et al., 1993; Balikhin and Gedalin, 1994; Gedalin et al., 1995a,b,c). If the ramp is narrow enough the electron motion in the inhomogeneous electric field becomes nonadiabatic and (at least some of the) electrons are demagnetized and accelerated across the magnetic field along the shock normal. It was shown (Balikhin and Gedalin, 1994; Gedalin et al., 1995a,b) that the immediate collisionless heating in this case is strong and the theoretically found correlations agree with the observed ones (Thomsen et al., 1987; Schwartz et al., 1988).

The nonadiabatic scenario was criticized (Scudder, 1995, 1996) as being inapplicable to the thoroughly studied "typical shock" (Scudder et al., 1986a,b,c). The basic argument was that the ramp is not sufficiently narrow to ensure the adiabaticity breakdown. However, recent analysis (Newbury

and Russell, 1996) have revealed that some shocks indeed possess extremely thin ramps $\sim c/\omega_{pe}$. For such small width the electron motion is no longer adiabatic. Moreover, it was shown (Gedalin et al., 1995b; Balikhin et al., 1997) that even in the substantially wider shocks some electrons become demagnetized nevertheless, and the resulting downstream distribution is produced both by adiabatic and nonadiabatic electrons, their relative importance being dependent on specific shock conditions. Detailed knowledge of the collisionless electron dynamics in the ramp is essential also for the determination which instabilities can grow and influence on the downstream electron distribution.

In contrast with the extensive analysis of electron demagnetization in the perpendicular shock front (Balikhin et al., 1993; Balikhin and Gedalin, 1994; Gedalin et al., 1995c), electron behavior in the oblique shock geometry is not understood equally comprehensively. The studied features include electron dynamics in a model geometry with a constant $\mathbf{B}$ and dependence of the single-particle energization on the initial phase (Gedalin et al., 1995b), topological analysis of the local stability criterion (Balikhin et al., 1997), and an example of electron heating in the conditions of strong demagnetization (Gedalin et al., 1995a). In the same time it is quite clear that perpendicular geometry is an exception. In oblique shocks the total energy an electron gains while crossing the ramp is equal to the de Hoffman-Teller cross-shock potential and is the same quantity for all electrons. This restriction does not exist for perpendicular shocks, which makes one expect that the electron energization in oblique shocks may look differently from what happens in the perpendicular limit.Yet it is quite obvious that any comparison with observational data requires at least semi-quantitative knowledge of the electron behavior in oblique shocks. In this and accompanying paper (Gedalin et al., 1998) we partially fill the gap in our knowledge of electron dynamics in oblique geometry.

The objective of the present paper is to study the dependence of the collisionless electron dynamics and downstream distribution on the shock width. In contrast with previous studies we do not consider only completely magnetized or strongly demagnetized limits but also pay attention to the regimes of partial demagnetization. The paper is organized as follows. In section 2 we briefly describe the transition from adiabatic to nonadiabatic electron motion. In section 3 we derive general local stability criterion in the shock front and analyze numerically the mostly nonadiabatic electron trajectories for the shock parameters close to those of the above "typical shock" while varying the ramp width. In doing so we consider electron motion only within the ramp, which is the only region in the shock front where demagnetization is possible (at least according to widely accepted stationary and one-dimensional shock model (Scudder et al., 1986a)). In section 4 we determine numerically and compare the downstream electron distributions obtained for different ramp widths.

2 Qualitative electron dynamics

Collisionless electron dynamics in the ramp is governed by the static electric and magnetic field:

$$\dot{\mathbf{v}} = -\frac{e}{m_e}(\mathbf{E} + \frac{\mathbf{v}}{c} \times \mathbf{B}), \tag{7}$$

where $\mathbf{E} = (E_x(x), E_y, 0), \mathbf{B} = (B_x, B_y(x), B_z(x))$, $E_y =$ const, $B_x =$ const, and x chosen along the shock normal, while y is the noncoplanarity direction. In the normal incidence frame (N, where the upstream plasma velocity is along the shock normal) $E_y = V_u B_{uz}/c$, where subscript u denotes upstream asymptotic values. In the de Hoffman-Teller frame (HT, where the upstream plasma velocity is along the upstream magnetic field) $E_y = 0$. The upstream magnetic field $\mathbf{B}_u = B_u(\cos\theta, 0, \sin\theta)$.

According to Gedalin et al. (1995b), if $|e(dE_x/dx)/m_e\Omega_e^2| \ll 1$, the electron motion combines a rapid gyration around the magnetic field, drift across the magnetic field, and acceleration along the magnetic field by the parallel component of the electric field. In this case the perpendicular energy of the electron increases adiabatically $v_\perp^2/B =$ const, while the HT cross-shock potential contributes to the total energy increase: $v_\parallel^2 + v_\perp^2 - 2e\varphi^{HT}/m_e =$ const. An electron which starts with low perpendicular energy $v_\perp \approx 0$ acquires almost all of the energy in the parallel degree of freedom.

If $-e(dE_x/dx)/m_e\Omega_e^2 \gtrsim 1$, the situation changes. The electron becomes effectively demagnetized and is dragged across the magnetic field by E_x, thus acquiring substantial energy in v_x. The above condition can be satisfied only in a part of the ramp, where $-(dE_x/dx) > 0$, and rapidly is broken when B becomes too high. Then the adiabatic gyration is restored, and the energy stored in v_x immediately transforms into the perpendicular (gyrational) energy. Thus, in this case an electron which starts with $v_\perp \approx 0$, utilizes a substantial part of the cross-shock potential as a direct input in the perpendicular degree of freedom.

When the conditions for the breakdown of adiabaticity are satisfied, the electrons with high initial $v_\perp$ still behave almost adiabatically, while only electrons with relatively low initial $v_\perp$ acquire substantial gyrational energy in the nonadiabatic way, so that the contribution of nonadiabatic electrons in the resulting electron heating depends on their percentage in the initial distribution: the higher the initial electron temperature, the weaker will be the role of the described demagnetization (Gedalin et al., 1995c; Scudder, 1996). This conclusion agrees with the observation (Schwartz et al., 1988) that strong heating occurs in shocks with relatively low v_{Te}/V_u. It is at least very difficult to estimate analytically the downstream distribution function in the case when at least part of the electrons become demagnetized. In the rest of the paper we use numerical methods to analyze the electron trajectories and the contribution of the demagnetized electrons in the downstream distribution and heating.

3 Single-particle behavior

Let us, following Balikhin et al. (1993), consider the local stability of an electron trajectory $\mathbf{r}(t), \mathbf{v}(t)$, trying small deviations $\delta\mathbf{r}(t), \delta\mathbf{v}(t)$, linearizing (7) near the trajectory, and assuming $\delta\mathbf{r}(t), \delta\mathbf{v}(t) \propto \exp(\lambda t)$. The evolution of these deviations is described by the following equation:

$$\begin{aligned}\lambda\delta\mathbf{v} &= -\frac{e}{m}\frac{d\mathbf{E}}{dx}\frac{\delta v_x}{\lambda} \\ &- \frac{e}{mc}\delta\mathbf{v}\times\mathbf{B} - \frac{e}{mc}\mathbf{v}\times\frac{d\mathbf{B}}{dx}\frac{\delta v_x}{\lambda},\end{aligned} \tag{8}$$

where we have taken into account that the fields depend only on x. It is easy to find the following equation for λ:

$$\begin{aligned}&\lambda^4 - \lambda^2[\alpha - \hat{\mathbf{n}}\cdot(\mathbf{v}\times\mathbf{\Omega}' - \mathbf{\Omega}^2] + \tfrac{1}{2}\lambda(\hat{\mathbf{n}}\cdot\mathbf{v})(\mathbf{\Omega}^2)' \\ &- (\hat{\mathbf{n}}\cdot\mathbf{\Omega})[\alpha(\hat{\mathbf{n}}\cdot\mathbf{\Omega}) + \mathbf{\Omega}'\cdot(\mathbf{v}\times\mathbf{\Omega})] = 0,\end{aligned} \tag{9}$$

where $\mathbf{\Omega} = (e/mc)\mathbf{B}$, $\mathbf{\Omega}' = d\mathbf{\Omega}/dx$, $\hat{\mathbf{n}} = (1,0,0)$, and

$$\alpha = -\frac{e}{m}\frac{dE_x}{dx}. \tag{10}$$

The trajectory is unstable if there exists a root λ such that $\Re\lambda > 0$. It is easy to see that the sufficient condition for such a root to exist is

$$\alpha(\hat{\mathbf{n}}\cdot\mathbf{\Omega}) + \mathbf{\Omega}'\cdot(\mathbf{v}\times\mathbf{\Omega}) > 0. \tag{11}$$

Although it is not difficult to meet the instability criterion (11) the criterion itself is not quite informative. First, in order that the instability to develop the growth rate should be large enough: $\lambda \gg v_x/L$, where L is the typical scale of the field inhomogeneity. Second, formally the instability occurs even in the absence of the electric field and for arbitrarily weak inhomogeneity (such $\mathbf{v}$ can be always found). Third, (11) provides only a local criterion, while real instability requires positive λ at least over a substantial part of the whole trajectory.

Global trajectory analysis of (7) is possible only in very special cases (Gedalin et al., 1995b), and we apply the numerical analysis of the electron trajectories in the model shock front. More specifically, we approximate the ramp by the following profile:

$$B_z = B_u \sin\theta\left[\frac{R+1}{2} + \frac{R-1}{2}\tanh\left(\frac{3x}{D}\right)\right], \tag{12}$$

where θ is the angle between the shock normal and magnetic field, B_u is the upstream magnetic field, R is the downstream-to-upstream B_z ratio, and D is (approximately) the ramp half width. For the noncoplanar magnetic field we use the expression derived by Gedalin (1996) (see also Jones and Ellison, 1987):

$$B_y = \frac{c\cos\theta}{M\omega_{pi}}\frac{dB_z}{dx}, \tag{13}$$

and approximate the cross-ramp electric field (in the normal incidence frame) by

$$eE_x^{(N)} = -\frac{1}{n}\frac{dp_e}{dx} - \frac{1}{8\pi n}\frac{dB^2}{dx}, \tag{14}$$

where we also assume $p_e \propto n^\gamma$, $\gamma = 2$, $n/B = \text{const}$. The first (pressure induced) term in (14) gives the de Hoffman-Teller cross shock potential. It should be noted that the adopted shape of the magnetic field slightly overestimates the field gradients (including the electric field) in the middle of the ramp, but underestimates dE_x/dx at the edges of the ramp. This form of the electric field, which has a sharp peak inside the ramp, is qualitatively consistent with the available high resolution electric field measurements on the bow shock (Wygant et al., 1987).

For the numerical analysis of single electron trajectory the following parameters were chosen: $M = 7.6$, $R = 6$, $\theta = 76°$, $2e\varphi^{(HT)}/m_iV_u^2 = 0.1$, and $2e\varphi^{(N)}/m_iV_u^2 = 0.26$. The ramp half-width D is measured in the electron inertial length c/ω_{pe} and varied in the range $2.5 - 5$. These parameters are close to the parameters of the "typical shock" by Scudder et al. (1986a,b,c), except the cross-ramp electric field, which could not be determined observationally with the same resolution.

As a characteristic of the ramp width significance we choose the trajectory of the electron which starts with the velocity $\mathbf{v}_0 = (V_u, 0, 0)$. There are several reasons for choosing this initial parameters as characteristic. First, adiabatic invariant conservation is broken more easily when the invariant itself is small. In this case the magnetic moment is identically zero, so this trajectory is among the first becoming nonadiabatic under inhomogeneous electric field. Second, analysis of the behavior of this particle shows what would happen with the cold electron distribution. Third, usual application of the Liouville mapping deals with the $v_\perp = 0$ section of the upstream and downstream electron distribution (Scudder et al., 1986c; Schwartz et al., 1988).

Figure 1 shows the changes in the electron behavior with the change of the ramp width. It is easily seen that the trajectory is always nonadiabatic, since the downstream $v_\perp \neq 0$. For the wide ramp the downstream gyrational energy is negligible. It rapidly increases with the decrease of the ramp width. The quantitative characteristics of this evolution is the fraction of the NIF cross-shock potential which goes into the electron gyrational energy. It drastically increases from 2% for $D = 5$ to 60% for $D = 2.5$. The last number means that a cold electron distribution would be heated extremely strongly in such a structure. In reality the electron distributions are hot, and $v_{Te} \gtrsim V_u$, so that heating study requires analysis of the whole distribution.

4 Heated distributions

In order to study the evolution of electron distributions across the shock as a function of the shock width, we trace the initial Maxwellian distribution (2000 particles) across the shock,

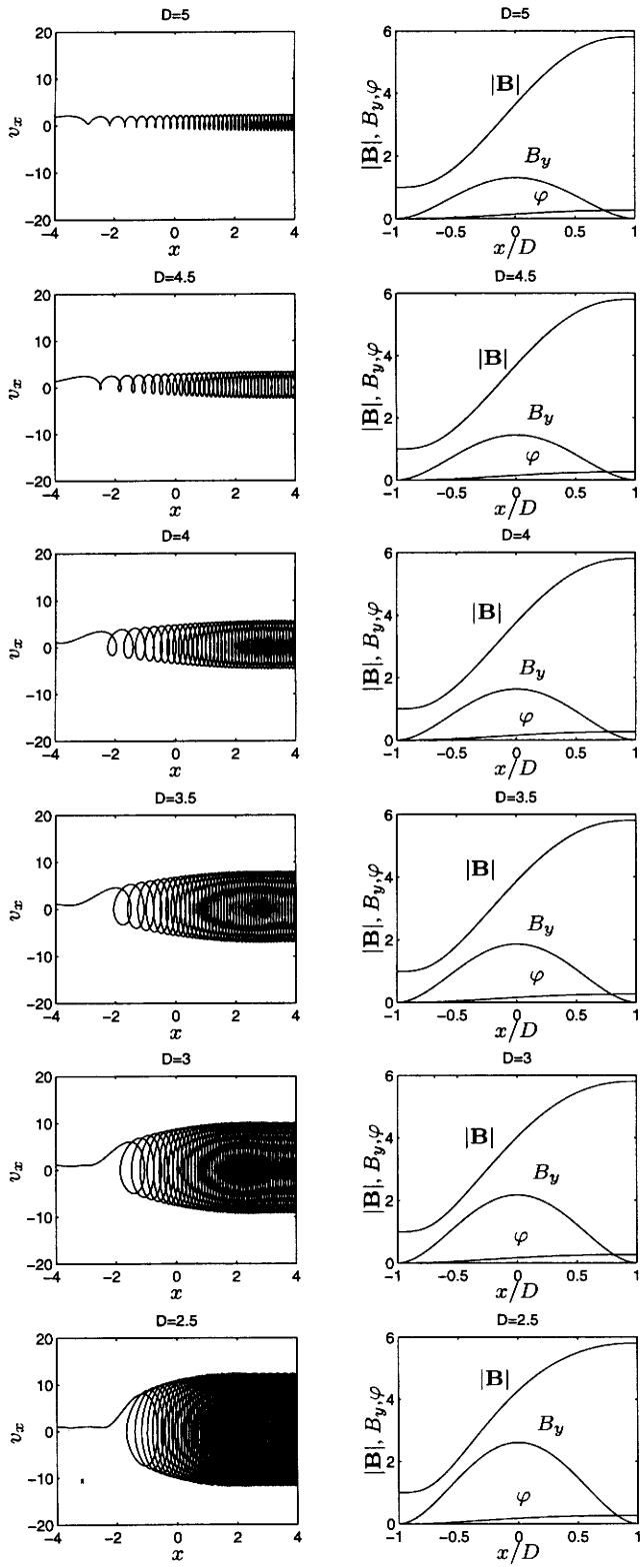

Fig. 1. Trajectory of the electron starting with the velocity $\mathbf{v}_0 = (V_u, 0, 0)$ for different ramp half-widths: 5, 4.5, 4, 3.5, 3, and 2.5 c/ω_{pe} (top to bottom). The right hand column shows the corresponding field profiles, used for numerical analysis.

and construct the downstream distribution using the staying time method (Veltri et al., 1990; Gedalin et al., 1995a,c). For the present analysis the following parameters were chosen: $B_{zd}/B_{zu} = 4$, $M = 7$, $v_{Te}/V_u = 3$, $\theta = 76°$, $e\varphi^{(HT)} = 0.2(m_i V_u^2/2)$, and $e\varphi^{(N)} = 0.45(m_i V_u^2/2)$. The ramp width D is measured this time in whistler lengths $l_W = \pi c \cos\theta / M\omega_{pi}$. In physical units the above parameters are as follows: $V_u = 400\, km/s$, $T_e = 4\, eV$, $e\varphi^{(HT)} = 180\, eV$, and $e\varphi^{(N)} \approx 400\, eV$.

There is a problem in representation of the downstream distribution function. The experimental ISEE device, producing the two dimensional distributions and their cuts, in fact provides the following function (cf. Feldman, 1985; Scudder, 1996):

$$F(\epsilon, \phi) = \int_{\epsilon}^{\epsilon+\Delta\epsilon} d\epsilon \int_{\theta_0}^{\pi-\theta_0} \sin\theta\, d\theta \int_{\phi}^{\phi+\Delta\phi} d\phi f(\epsilon, \theta, \phi), \tag{15}$$

where $\theta_0 = 55°$ is the fan opening angle, $\Delta\epsilon/\epsilon = 0.29$, and θ and ϕ are spherical coordinates when z axis is along the axis of 3s period rotation of the spacecraft. It is easily seen that even when assuming $\Delta\phi \to 0$, $\Delta\epsilon \to 0$, and the distribution is gyrotropic with the magnetic field along z axis, the deconvolution of the true distribution function is not immediate, in contrast with what is claimed by Scudder (1996). The situation is even more complicated when the gyrotropy axis does not coincide with the spacecraft rotation axis, and the magnetic field direction changes on the time scale of the rotation period 3s, during which data for one distribution has been collected.

Since the three dimensional distribution is impossible to represent, for the present case we adopted the following representation

$$F(v_\parallel, v_\perp) = \int f(v_\parallel, v_{\perp,1}, v_{\perp,2}) dv_{\perp,2}, \tag{16}$$

where $v_{\perp,1}$ and $v_{\perp,2}$ are two components of the velocity, perpendicular to the magnetic field. It should be understood that this distribution function cannot be directly compared to the observational data either. However, it allows to demonstrate quite clearly the difference between the adiabatic and nonadiabatic cases.

The above defined and numerically obtained distribution function is shown in Figure 2 for different ramp widths. It is easily seen that the adiabatic accelerated beam (for $D = 1.8 l_W$) is smoothed to a wide distribution function in the case of strong demagnetization (for $D = 0.8 l_W$). For the more quantitative assessment the following parameters were calculated: efficiency $\Delta T_\perp/(m_i V_u^2/2)$, which shows how much of the initial flow energy is utilized in the perpendicular heating, overadiabaticity $T_\perp/(T_u B_d/B_u)$, which shows how stronger is the heating relative to the static magnetic compression, and parallel preheating $T_\parallel/T_u$, which describes the widening of the electron beam in the parallel direction. The last parameter is not the eventual parallel heating since there is still a gap which should be filled and that would affect the

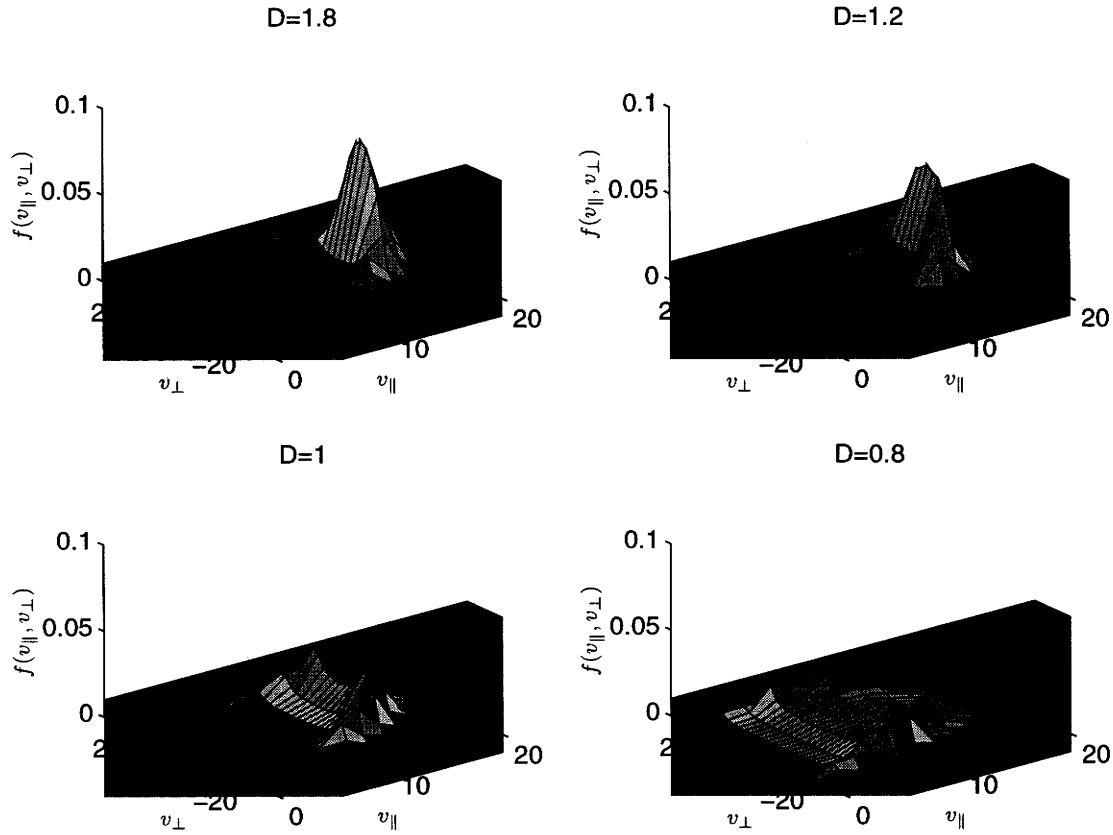

Fig. 2. Two-dimensional projection (16) for different ramp widths: $D = 1.8l_W$ (completely adiabatic), $D = 1.2l_W$, $D = 1l_W$, and $D = 0.8l_W$ (strong demagnetization).

Table 1. Collisionless electron preheating efficiency for different ramp widths

Ramp Width $D/(\frac{\pi c \cos\theta}{M\omega_{pi}})$	Efficiency $\Delta T_\perp/\frac{1}{2}m_i V_u^2$	Overadiabaticity $T_\perp/T_u(\frac{B_d}{B_u})$	Parallel Preheating $T_\parallel/T_u$
1.8	0.01	1.1	0.6
1.2	0.02	1.4	0.5
1.0	0.04	2.2	0.9
0.8	0.07	3.9	1.6

final temperature. The calculated parameters are given in Table 1. One can easily see that the (partial) demagnetization of electrons in the narrow ramp not only results in the strong immediate heating in the perpendicular direction, but is also accompanied by significant preheating in the parallel direction.

5 Conclusions

In the present paper we analyzed the dependence of the electron dynamics in the shock front and the corresponding downstream distribution on the ramp width. We studied the trajectory of the central particle of the distribution (the one which moves with the plasma flow velocity before the ramp) and found that the gyration energy that this particle can get from the cross-shock potential, rapidly increases with the decrease of the ramp width. This does not immediately mean that the whole distribution heats efficiently, especially when the initial temperature is high. However, we found that the downstream distribution also changes drastically when the ramp becomes narrow: the narrower the ramp, the higher is the efficiency of the utilization of the cross-shock potential into the perpendicular degree of freedom.

Several comments should be added. First, we considered only the electron behavior at the ramp, and did not take into account the other parts of the structured shock front (foot, overshoot, precursor, downstream large amplitude oscillations). This has been done because either the typical scales of these parts are large of the corresponding potentials are insufficient to result in substantial demagnetization. Therefore, the electron dynamics and evolution of the electron distribution in these parts of the shock follow the adiabatic prescription where $v_\perp^2/B \approx$ const. This adiabatic evolution affects the final distribution shape but does not affect the demagnetization properties which are determined only by the fields in the ramp (unless there are other regions where sufficiently sharp gradients of the quasistatic electric field exist).

The model fields, used in the numerical analysis, are not thought to be directly applied to any specific shock. Nor are the found values of perpendicular and parallel heating.

One has to know with confidence the quasi-stationary fields in the shock front to make reliable *quantitative* estimates. The above analysis provides the semi-quantitative conclusions about the dependence of the electron dynamics and heating on the shock scale. These semi-quantitative predictions may become comparable with observations when better electric field measurements are available.

Second, the usage of the static fields throughout may be a little misleading, since the analysis required only that the fields be stationary on the typical electron time, that is, that the characteristic time of the field variation be much larger than the electron gyroperiod. That means that even if the shock is nonstationary and the profile changes at the ion gyroperiod scale, from the electron dynamics (in the ramp) point of view it is still governed by quasistatic fields. In this case, of course, (12)–(14) are no longer good approximations at large spatial and temporal scales, although they may appear quite appropriate for the field description at the spatial scale of the ramp and temporal scale of ion gyroperiod. This issue requires better knowledge about the shock structure and is beyond the scope of the present paper.

Third, the collisionless heating alone cannot, apparently, provide the observed smooth downstream distribution without gaps, which are predicted by either of the collisionless heating models. The final work has to be done by instabilities. If this smoothing is done at the spatial scale of the ramp, the instabilities have to be fast. In this case the very existence of an instability and its growth rate are primarily determined by the electron distribution in the ramp and is thus affected also by possible demagnetization. Alternative (may be complementary) mechanism should be via slight nonstationarity of the shock front and rippling of the shock surface, due to which the electrons coming from different entries into the ramp mix downstream to smooth the distribution. These questions are beyond the scope of the present paper.

Acknowledgements. The research was supported in part by Israel Science Foundation under grant No. 261/96-1.

References

Balikhin, M., Krasnosel'skikh, V.V., Woolliscroft, L.J.C., and Gedalin, M., A study of the dispersion of the electron distribution in the presence of E and B gradients: application to electron heating at quasi-perpendicular shocks, *J. Geophys. Res.*, in press (1998).

Balikhin, M., Gedalin, M., and Petrukovich, A., New mechanism for electron heating in shocks, *Phys. Rev. Lett., 70*, 1259-1261, 1993.

Balikhin, M. and Gedalin, M., Kinematic mechanism for shock electron heating: comparison of theoretical results with experimental data, *Geophys. Res. Let., 21*, 841-844, 1994.

Feldman, W.C., Electron velocity distributions near collisionless shocks, in *Collisionless Shocks in the Heliosphere: Reviews of Current Research, Geophys. Monogr. Ser.*, vol. 35, edited by R.G. Stone and B.T. Tsurutani, pp. 195–205, AGU, Washington, D. C., 1985.

Gedalin, M., Balikhin, M., and Krassnoselskikh, V., Electron heating in collisionless shocks, *Adv. Space Res., 15(8/9)*, 225–233, 1995a.

Gedalin, M., Gedalin, K., Balikhin, M., and Krasnoselskikh, V.V., Demagnetization of electrons in the electromagnetic field structure, typical for oblique collisionless shock front, *J. Geophys. Res., 100*, 9481–9488, 1995b.

Gedalin, M., Gedalin, K., Krasnoselskikh, V.V., Balikhin, M., and Woolliscroft, L.J.C., Demagnetization of electrons in inhomogeneous $\mathbf{E} \perp \mathbf{B}$: Implications for electron heating in shocks, *J. Geophys. Res., 100*, 19,911–19,918, 1995c.

Gedalin, M., Noncoplanar magnetic field in the collisionless shock front, *J. Geophys. Res., 101*, 11,153–11,156, 1996.

Gedalin, M., Griv, E., and Balikhin, M.A., Width dependent collisionless electron dynamics in the static field of the shock ramp, 2, Phase space portrait, (this issue).

Jones, F.C., and Ellison, D.C., Noncoplanar magnetic fields, shock potentials, and ion deflection, *J. Geophys. Res., 92*, 11,205–11,207, 1987.

Newbury, J.A. and Russell, C.T., Observations of a very thin collisionless shock, *Geophys. Res. Lett., 23*, 781-784, 1996.

Schwartz, S.J., Thomsen, M.F., Bame, S.J., and Stansbury, J., Electron heating and the potential jump across fast mode shocks, *J. Geophys. Res., 93*, 12,923–12,931, 1988.

Scudder, J.D., A review of the physics of electron heating at collisionless shocks, *Adv. Space Res., 15*(8/9), 181–223, 1995.

Scudder, J.D., Comment on "Demagnetization of electrons in inhomogeneous $\mathbf{E} \perp \mathbf{B}$: Implications for electron heating in shocks" by M. Gedalin et al., *J. Geophys. Res., 101*, 2560–2563, 1996.

Scudder, J.D., Mangeney, A., Lacombe, C., Harvey, C.C., Aggson, T.L., Anderson, R.R., Gosling, J.T., Paschmann, G., and Russell, C.T., The resolved layer of a collisionless, high β, supercritical, quasi-perpendicular shock wave, 1, Rankine-Hugoniot geometry, currents, and stationarity, *J. Geophys. Res., 91*, 11,019–11,052, 1986a.

Scudder, J.D., Mangeney, A., Lacombe, C., Harvey, C.C., and Aggson, T.L., The resolved layer of a collisionless, high β, supercritical, quasi-perpendicular shock wave, 2, Dissipative fluid electrodynamics, and stationarity, *J. Geophys. Res., 91*, 11,053–11,073, 1986b.

Scudder, J.D., Mangeney, A., Lacombe, C., Harvey, C.C., Wu, C.S., and Anderson, R.R., The resolved layer of a collisionless, high β, supercritical, quasi-perpendicular shock wave, 3, Vlasov electrodynamics, *J. Geophys. Res., 91*, 11,075–11,097, 1986c.

Thomsen, M.F., Mellott, M.M., Stansbury, J.A., Bame, S.J., Gosling, J.T., and Russell, C.T., Strong electron heating at the Earth's bow shock, *J. Geophys. Res., 92*, 10,119–10,124, 1987.

Veltri, P., Mangeney, A., and Scudder, J.D., Electron heating in quasiperpendicular shocks: A Monte-Carlo simulation, *J. Geophys. Res., 95*, 14,939–14,959, 1990.

Veltri, P. and Zimbardo, G., Electron - whistler interaction at the Earth's bow shock. 1. Whistler instability, *J. Geophys. Res., 98*, 13,325–13,333, 1993a.

Veltri, P., and Zimbardo, G., Electron - whistler interaction at the Earth's bow shock: 2, Electron pitch angle diffusion, *J. Geophys. Res., 98*, 13,335–13,346, 1993b.

Wygant, J.R., Bensadoun, M., and Mozer, F.C., Electric field measurements at subcritical, oblique bow shock crossings, *J. Geophys. Res., 92*, 11,109–11,121, 1987.